CORE ANALYSIS BY LOW FIELD NMR

Christian Straley, Dan Rossini (Schlumberger-Doll Research Center)
Harold Vinegar, Pierre Tutunjian (Shell Development Co.)
Chris Morriss (Schlumberger Wireline and Testing)

Abstract

NMR core measurements have been made customarily in high magnetic fields, emphasizing T_1 for pore-size evaluation or using chemical shift spectroscopy for quantitative differentiation of oil and water. However, new NMR logging tools use T_2 measurements made at low field strengths and these measurements should be supported by core analysis. This paper illustrates that low field NMR T_2 measurements made on water-saturated rock cores can be used to measure total porosity and extract T_2-distributions. The T_2-distributions are shown to be closely related to pore size distributions. Our experiments demonstrate that low field measurements are quantitative, even for cases where high field measurements fail. T_2-distributions from water-saturated plugs are used to estimate producible fluids for sandstones and carbonates and to estimate clay bound water and matrix permeability. Although chemical shift spectroscopy is not feasible at low fields, a method is demonstrated on *native state* diatomites that permits the measurement of oil, water and gas saturation. In the case presented, it is also possible to determine the oil viscosity, in situ.

Introduction

Hydrogen (^{1}H) nuclear magnetic resonance (NMR) is a rapid, nondestructive measurement that can provide a wealth of information about the fluids in oil- and water-saturated rock. This paper illustrates many applications of low field NMR measurements to core analysis. Low field NMR has been found to be more accurate in measuring water and oil volumes than high field NMR for rocks that have large internal magnetic field gradients. Moreover, low field measurements are of great interest since the new pulsed NMR logging tools [1, 2, 3] are able to generate fields only in the range 120 to 550 gauss.

Low field NMR measures three properties, the equilibrium nuclear magnetization, M_n, and the two principal NMR relaxation times, T_1 (the longitudinal relaxation time) and T_2 (the transverse relaxation time). M_n is proportional to the *fluid-filled* porosity while T_1 and T_2 have been correlated with petrophysical properties such as pore size, producible fluid and permeability. Although T_1 measurements are more common in the literature, they are more time consuming to measure than T_2 measurements. Hence, the new pulsed NMR logging tools preferentially measure T_2 for faster logging speeds and increased wellsite efficiency.

Traditionally, quantitative analysis by NMR has used high field rather than low field measurements. The use of high field, H, increases the available signal as indicated by its relationship to the nuclear magnetization,

$$M_n = \chi_n H, \tag{1}$$

where χ_n is the static nuclear susceptibility due to the hydrogen. Higher magnetic fields result

in a stronger signal, hence greater signal-to-noise ratio and faster measurements. At higher field, larger chemical shifts permit differentiation of oil and water signals. [4].

For fluids in porous media, however, the increased field that improves the signal also causes higher internal gradients, G, that degrade the measurements [5]. When a rock is in an applied field, the gradients arise from magnetic field inhomogeneity, ΔH, due to the susceptibility contrast between rock grains and pore fluids,

$$\Delta H \approx \Delta \chi_e H, \tag{2}$$

where $\Delta \chi_e$ is the difference in susceptibilities (due primarily to electronic contributions). In rocks, the internal gradients resulting from field inhomogeneity are a complicated function of microgeometry but are on the order of ΔH divided by the grain size. G can frequently exceed 100 gauss/cm at 20 kilogauss (85 MHz ^{1}H Larmor frequency). The same rocks would have gradients of only 2.5 gauss/cm at 500 gauss (2.1 MHz ^{1}H Larmor frequency).

To understand why large internal magnetic field gradients can cause complications it is necessary to consider the three T_2 relaxation mechanisms in rocks. These are due to (1) molecular motion in fluids, (2) surface relaxivity at the pore wall and (3) molecular diffusion in the internal gradients.

The first mechanism, due to local motions such as molecular tumbling, is equally effective whether or not the fluid is in a rock. This is called *bulk liquid* relaxation. The bulk liquid T_2 decreases as fluid viscosity, η, increases [6],

$$T_{2B} \sim \frac{T}{\eta}, \tag{3}$$

where T is the absolute temperature.

The second mechanism is the relaxation of ^{1}H nuclei when they closely approach paramagnetic ions such as iron or manganese, which reside on grain surfaces. Fluid molecules diffuse to the surface, have a probability of being relaxed there, and then diffuse away. For water in an individual pore the relaxation time constant is [7]

$$T_{2S} = \frac{1}{\rho_2}(\frac{V}{S}), \tag{4}$$

where (S/V) is the surface-to-volume ratio of the pore and ρ_2 is the transverse surface relaxivity.

The third mechanism is due to the diffusion of molecules in magnetic field gradients. Using the Carr-Purcell-Meiboom-Gill (CPMG) pulse sequence, the relaxation time due to diffusion (T_{2D}) is

$$T_{2D} = \frac{3}{\gamma^2 G^2 D \tau^2} \tag{5}$$

where γ is the ^{1}H gyromagnetic ratio, D is the diffusion coefficient and τ is the Carr-Purcell pulse spacing. The CPMG sequence produces a closely-spaced train of spin echoes whose decay is analyzed to determine T_2. The interecho spacing, 2τ, can be varied and is an important experimental parameter [8, 9].

The time dependence of the signal, A(t), from all three processes and measured at the peaks of the echoes, is [8, 10]

$$A(t) = A(0)e^{-t/T_{2B}}e^{-t/T_{2S}}e^{-\gamma^2G^2D\tau^2t/3}. \quad (6)$$

A(0), the signal at time = 0, is proportional to M_n and therefore fluid-filled porosity. For quantitative analysis A(0), T_{2B} and T_{2S} are of interest; the gradient diffusional relaxation is considered a nuisance. In rocks with potentially high internal gradients, e.g. very shaly sands (or measurements made at high field), the extrapolation to find A(0) can be inaccurate and the relaxation curves for the bulk fluid or surface relaxation can be completely obscured. Fortunately, the relaxation due to the gradients can be minimized by shortening τ as seen in Equation 6. However, because of spectrometer hardware constraints at high field it is not always possible to achieve the required interecho spacing and for many rocks it is better to work at low magnetic field strengths (where G is also smaller).

For the purposes of this paper, low field means a CPMG sequence with $H\tau \approx 0.1$ gauss-sec. Consider the extreme case of water ($D = 2 \times 10^{-5}\ cm^2/sec$) in an internal gradient of 10 gauss/cm (due to a 500 Gauss applied field). If $H\tau = 0.1$ gauss-sec is maintained, gradient diffusional relaxation will be negligible for T_2 values as high as that of bulk water. When gradient diffusional relaxation is negligible, T_1 and T_2 contain the same petrophysical information, and the ratio of T_1 to T_2 has been shown to be approximately 1.6 for a collection of sandstones and carbonates [8].

NMR transverse relaxation data can be expressed as a sum of exponentials

$$A(t) = \sum_i A(0)_i e^{-t/T_{2i}}. \quad (7)$$

Equation 7 can be inverted into a T_2 relaxation time distribution, where the T_{2i} are a preselected basis set of relaxation time constants and the $A(0)_i$ are the signal amplitudes associated with each time constant by fitting [11, 12, 13].

Single component fluids are characterized by a single value of T_2. For example, bulk water has a T_2 of 3 sec at room temperature. Multicomponent fluids such as crude oils often display a distribution of relaxation times [14].

In water-saturated rocks, the bulk water relaxation is often negligible, and the distribution of T_2 arises from the distribution of surface-to-volume ratio of the pores (as shown in Equation 4) [9]. Because T_2 depends linearly upon pore size, the T_2-distribution corresponds to a pore size distribution with the largest pores having the longest relaxation times.

When oil and water coexist in the pore space, the general principle is that the relaxation of fluid in contact with grain surfaces is enhanced by those surfaces. See Equation 4. Conversely, fluid that does not wet the surface relaxes at its bulk rate, as relaxation does not occur at the oil-water interface. Because oil and water have similar ^1H density, the T_2-distribution is a linear summation of the individual contributions from the oil and water.

Results and Discussion

Porosity

Evidence of internal gradients and their dependence on magnetic field can be seen in porosity measurements on a suite of shaly sands and shales from the Shell Johnson City test well. Figure 1 compares porosity measurements made at 85, 2 and 1 MHz with Carr-Purcell pulse spacing (τ) of 0.25, 0.08 and 0.25 msec, respectively. These values of τ were the shortest that could be achieved with the instruments. The unknown porosity, $\phi_{unknown}$, is determined by comparing the signal, $A(0)_{unknown}$ from Equation 6, to the values for a standard sample.

$$\phi_{unknown} = \frac{A(0)_{unknown}}{A(0)_{standard}} \times \phi_{standard} \tag{8}$$

The 85 MHz data were collected on a GE CSI-2T spectrometer, the 2 MHz data on a custom-built Schlumberger spectrometer and the 1 MHz data on the NUMAR CoreSpec 1000.[1]

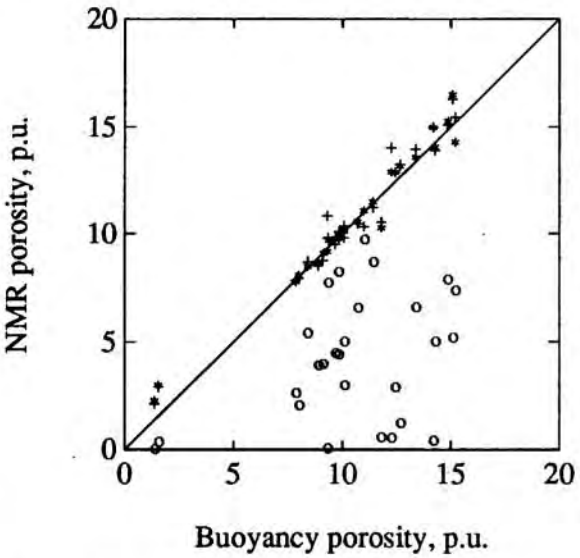

Figure 1: Comparison of NMR porosity measured at three field strengths to buoyancy porosity. o is 85 MHz data, + is 2 MHz data, * isl MHz data.

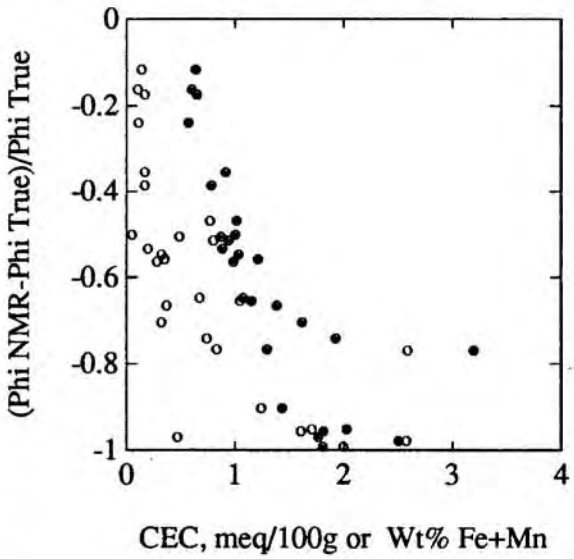

Figure 2: The relative error in 85 MHz NMR porosity crossplotted with CEC and paramagnetic impurities. The open circles indicate CEC values and the solid circles are weight percent Fe plus Mn.

Clearly, the porosity from the 85 MHz measurement significantly underestimated the gravimetric porosity for all of the samples, whereas the porosities from the 1 MHz measurement are in good agreement even though the same value of τ was used. As expected, due to the low field and very short τ values, the 2 MHz porosities are also in good agreement with gravimetric values.

The fractional error in the 85 MHz porosity is strongly correlated with the weight of paramagnetic impurities (iron and manganese) and similarly with the cation exchange capacity

[1] Mark of NUMAR Corp.

(CEC) values (Figure 2). This is expected since iron and manganese, the most common paramagnetic impurities and largest contributors to grain susceptibility, are often associated with clay minerals. Clay minerals have large surface area and high magnetic susceptibilities leading to large internal gradients and extremely short values of T_2.

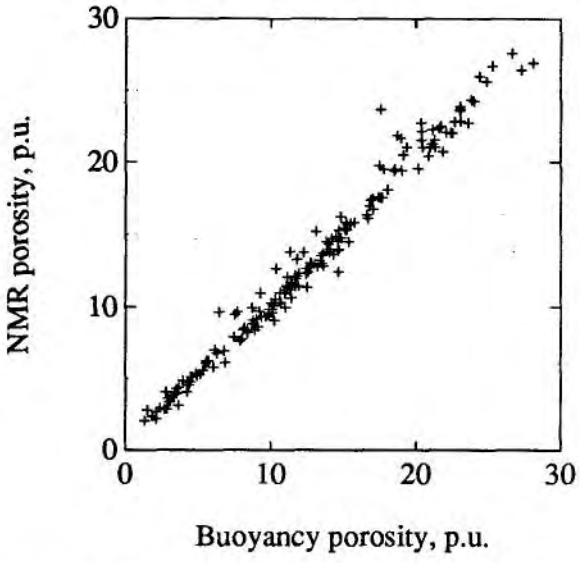

Figure 3: Comparison of 2 MHz NMR porosity with buoyancy porosity for 192 sandstones.

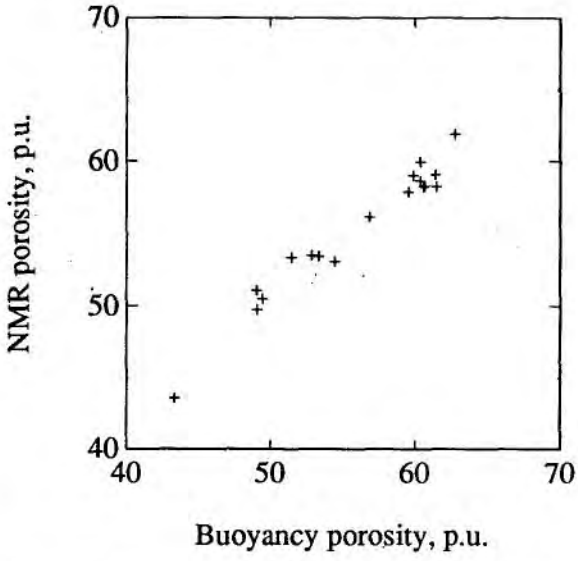

Figure 4: Comparison of 2 MHz NMR porosity with buoyancy porosity for 18 high porosity diatomites.

At low field, porosity can be accurately measured for both sandstones and carbonates. This is illustrated in Figures 3, 4 and 5 where 2 MHz NMR porosities are compared with gravimetric porosities for 281 samples.

The sandstone suite has 210 samples, including 18 diatomite plugs with porosities ranging from 45 to 65 p.u. The regression has a slope of 0.98, intercept of 0.5 p.u., and standard deviation of 0.8 p.u. A significant source of experimental error is the nonuniform sample size.

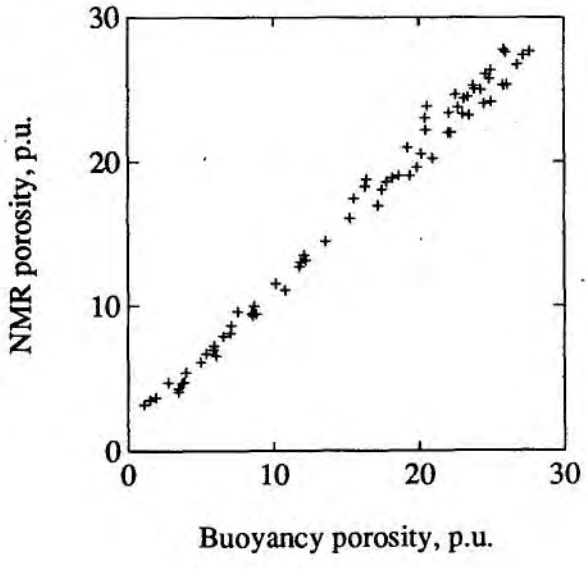

Figure 5: Comparison of 2 MHz NMR porosity with buoyancy porosity for 71 carbonates.

There are 71 carbonate samples. The regression has a slope of 0.97, intercept of 1.4 p.u., and standard deviation of 0.8 p.u. The higher intercept is due to two factors. First, about one third of the samples were known to be incompletely cleaned of hydrocarbons. This residual hydrocarbon is included in the NMR measurement, but not the gravimetric measurements. Second, many of the samples have surface vugs that were not completely dried prior to the NMR measurements.

Pore Size Distributions

T_2-distributions from low field CPMG data are similar to T_1-distributions and to pore size distributions from mercury porosimetry measurements [3, 8, 14]. T_1- and T_2-distributions for four sandstone samples from different formations are displayed in Figure 6 to illustrate the similarity. The T_1-distributions shown in Figure 6 have been shifted to shorter times using a factor of 2/3. This shift is required to roughly compensate for the different surface relaxivity for T_1 and T_2 processes.

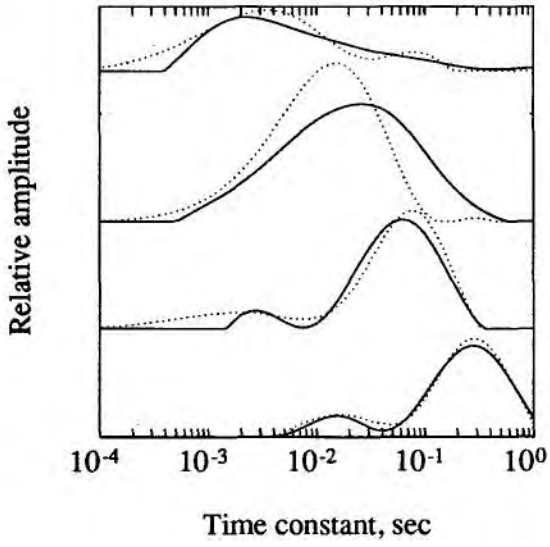

Figure 6: T_2- (dotted) and T_1-distributions (solid) for four sandstones measured at 2 MHz. The T_1 curves have been shifted by a factor of 2/3.

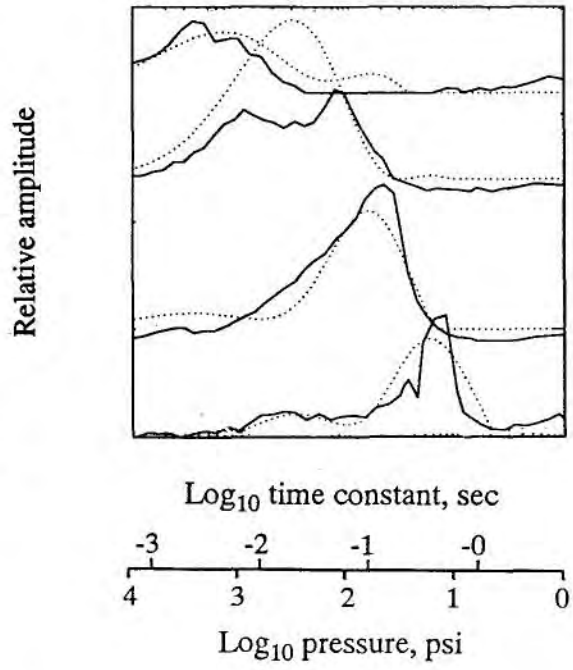

Figure 7: Differential mercury injection curves (solid) with the T_2-distributions (dotted) for the samples shown in the previous figure.

Figure 7 compares T_2-distributions and differential mercury capillary pressure curves for the same four sandstone samples. The curve overlay is based on a correspondence of $T_2P = 5.33$ sec-psi. Similar results have been reported for other sandstones and diatomite samples [3, 14].

Free Fluid Porosity

T_2-distributions can be used to estimate the volume of producible fluid in a manner similar to that described for T_1-distributions [15]. The NMR estimate of producible porosity is usually referred to as the free fluid porosity, or free fluid index.

This technique is based on an expectation that the producible fluids reside in the larger pore spaces, whereas the bound fluids are held in the smaller pores. Hence a T_2 cutoff (i.e., a pore size cutoff) may be applied to the T_2-distribution that divides the total NMR porosity into bound and free fluid porosity. The value of the T_2 cutoff is determined by the best agreement between the free fluid porosity and the volume of fluid that is centrifuged from the sample at 100 psi air-brine equivalent capillary pressure. Good agreement is obtained with cutoff values of 33 msec and 92 msec for sandstones and carbonates, respectively. Results are shown in Figures 8 and 9 for 86 sandstone and 25 carbonate samples.

T_2-distributions obtained for samples after centrifuging show that the bound, or irreducible, fluids are held in the small pores that have short T_2 values. For example, Figure 10 compares T_2-distributions for a sandstone sample before and after centrifugation under air. After centrifuging, the longest T_2 values correspond roughly to the 33 msec cutoff.

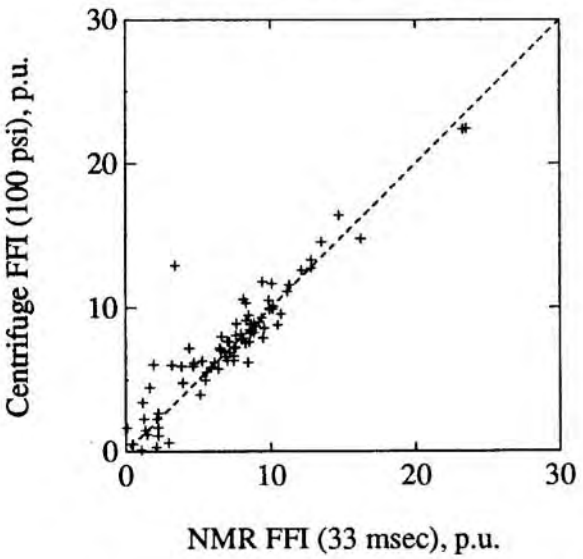

Figure 8: The volume of fluid expelled by centrifuging at 100 psi vs. air plotted against the NMR free fluid porosity calcuated using a 33 msec cutoff for a suite of sandstones. The dashed line is 1:1.

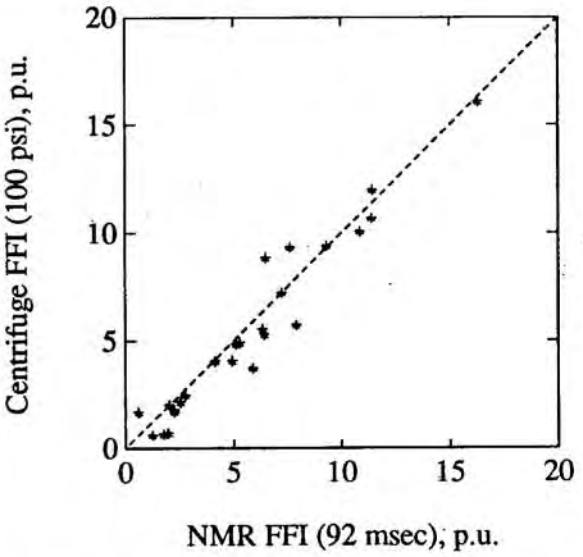

Figure 9: The volume of fluid expelled by centrifuging at 100 psi vs. air plotted against the NMR free fluid porosity calculated using 92 msec cutoff for a suite of carbonates. The dashed line is 1:1

Clay Bound Water

Estimation of clay bound water volume from the T_2-distribution is based on an assumption that clay bound water has the shortest T_2 values in the distribution; clays have high surface area and small pores. Hence, the pore volume with T_2 values shorter than a certain cutoff can be correlated with clay bound water estimates from electrical or other measurements.

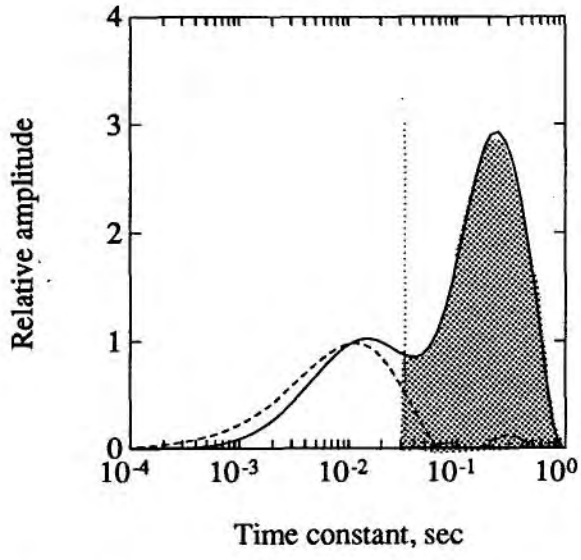

Figure 10: A vertical cutoff on a T_2-distribution separating the distribution into the long-T_2 porosity (shaded) and the short-T_2 porosity. The solid curve is the distribution for a fully saturated sandstone. The dashed curve shows the same sample after centrifuging at 100 psi vs. air. The dotted vertical line is located at a cutoff of 33 msec. The long-T_2 porosity found in this manner is called the free fluid porosity.

Cation exchange capacity/pore volume (Q_{ve}) was determined from electrical membrane potential measurements [16] for 45 oilfield sandstones from North America, South America and Europe. Clay bound water volumes were then calculated from the Q_{ve} values using the Hill-Klein-Shirley equation [17]. Comparing these bound water volumes with the cumulative porosity along the distribution, the best agreement with Q_{ve} measurements occurs at a cutoff of 3 msec (see Figure 11). This results in a minimum error of 0.75 p.u. A crossplot of the NMR estimate versus clay bound water is shown in Figure 12. These NMR measurements were made at 2.1 MHz using $\tau = 80$ μsec.

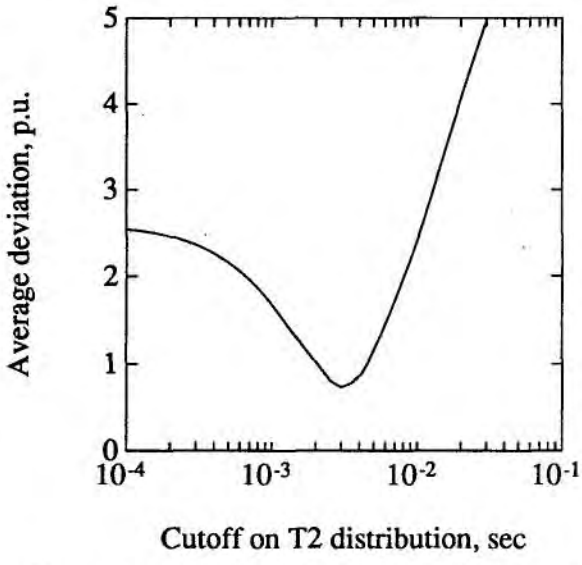

Figure 11: The minimum in the average deviation, at 3 msec, indicates the best agreement between clay bound water volume from membrane potential measurements and the T_2-distribution porosity for the smallest pores.

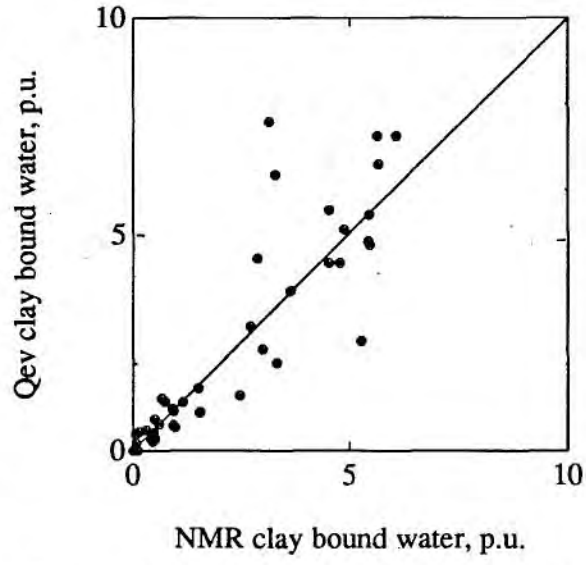

Figure 12: The clay bound water volume from membrane potential measurements compared with the cumulative porosity up to 3 msec on the T_2-distributions.

Permeability

$k = T_1^2\phi^4$ and similar expressions have been used to estimate matrix permeability in sandstones [18]. Applying this equation with porosity as a decimal fraction and T_1 in msec gives permeability estimates in md. Analogously, permeability may be estimated using

$$k = CT_{2ML}^2\phi^4. \tag{9}$$

The logarithmic mean T_2, T_{2ML}, is the value of T_2 that bisects the area under the T_2-distribution curve and is given by

$$T_{2ML} = exp(< logT_2 >) = exp(\frac{\Sigma\phi_i logT_{2i}}{\Sigma\phi_i}). \tag{10}$$

The NMR permeability estimate, using Equation 9 and a premultiplier (C) of 4.6, gives good agreement with air permeability for 110 sandstones from three reservoirs (Figure 13). Better agreement can be obtained by adjusting the premultiplier for each reservoir. The improvement using the NMR estimate rather than porosity alone is evident from a comparison of Figures 13 and 14.

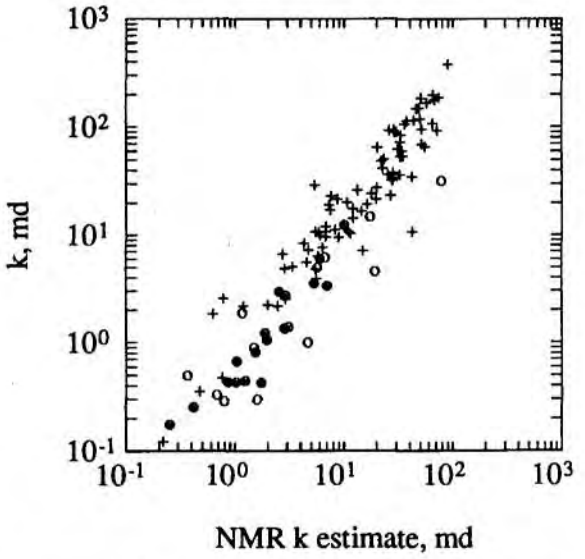

Figure 13: The measured permeability for three sandstone suites versus the permeability estimated by $4.6T_{2LM}^2\phi^4$.

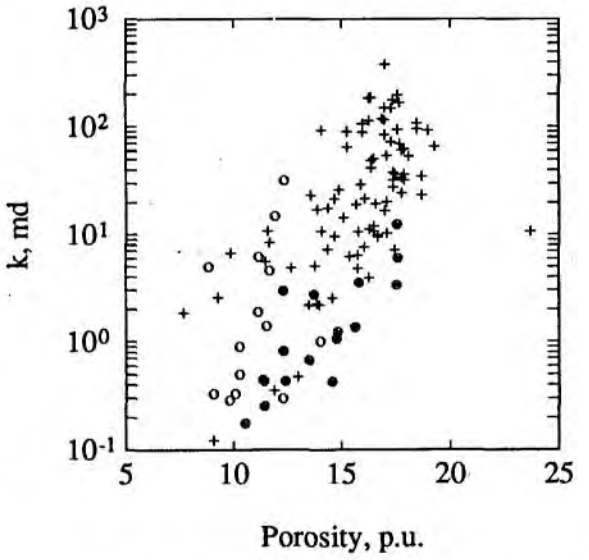

Figure 14: Permeability plotted against the total porosity for the three sandstone suites used in the previous plot.

In vuggy carbonates, a straightforward application of Equation 9 results in more scatter due to a greater variation in pore-body to pore-throat ratio. Use of the T_2-distribution allows discrimination of the separated vuggy porosity, which has a weak contribution to the permeability [19]. Figure 15 shows the permeability computed from Equation 9, for 23 vuggy dolomite samples from the Clearfork formation, using an upper T_2-cutoff of 750 msec. That is, values of both porosity and T_{2ML} are computed from that portion of the distribution below 750 msec. The dolomite samples are the same samples described in the free fluid porosity section. By using a truncated T_2-distribution, rather than the entire distribution, the error in permeability estimation was reduced from a factor of 4.8 to a factor of 2.6, as shown in Figure 16.

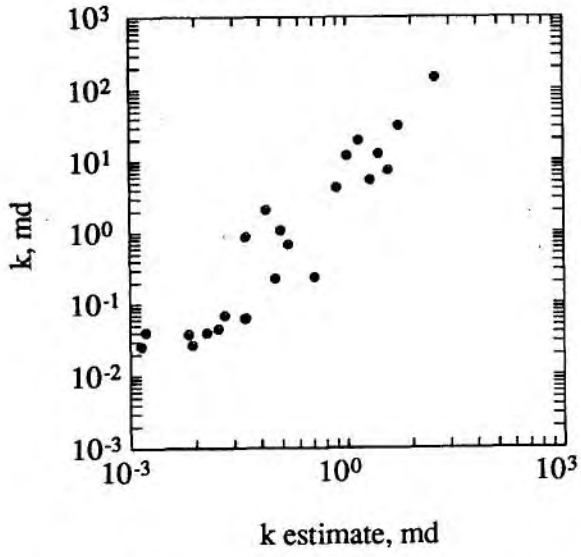

Figure 15: Crossplot of the NMR permeability estimate and the measured permeabilities for 23 Clearfork dolomites. This estimate is from the short-T_2 portion of the distribution that yielded the smallest error (see next figure).

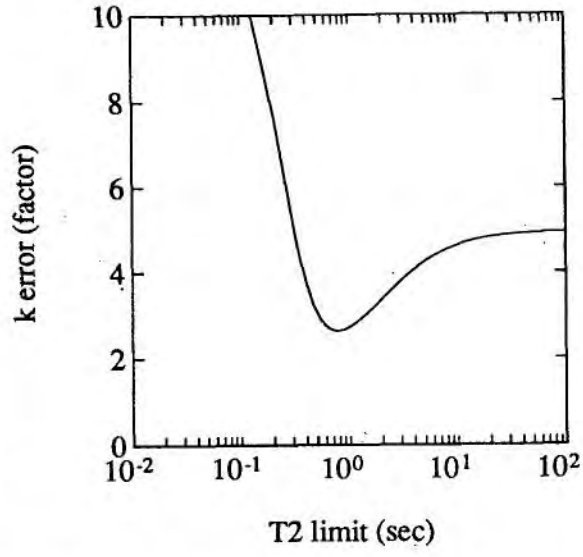

Figure 16: Variation in error from loglog crossplots of the measured permeability vs. the NMR estimate calculated using a limited extent of the distributions (as indicated on the x-axis).

Oil Viscosity

T_2-distributions were determined for 64 bulk oil samples and values of T_{2ML} determined from their distributions. Many of these crudes could not be characterized by a single time constant and T_{2ML} is used to approximate T_{2B}. As expected from Equation 3, values of T_{2ML} vary inversely with oil viscosity (see crossplot, Figure 17). The best fit of the data from 0.7 to 1000 cp is given by $T_{2ML} = 1.200/\eta^{0.9}$.

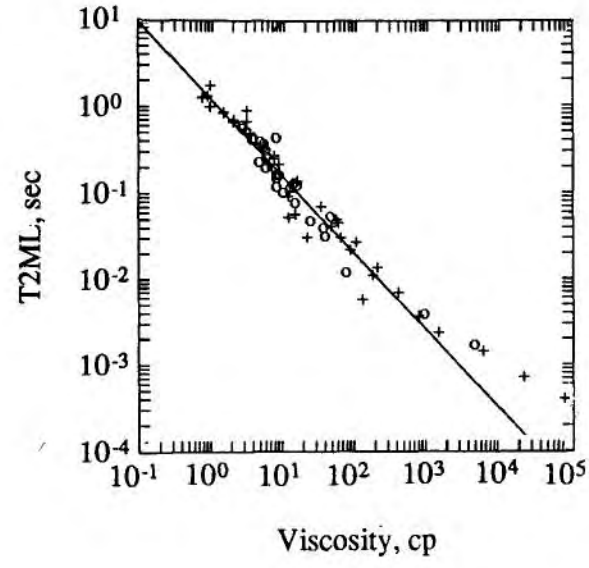

Figure 17: The measured oil viscosity is plotted against T_{2ML}. Belridge samples are indicated by o and other oil samples are indicated by +. The fit (solid line), for the data from 0.7 to 1000 cp, is given by a power law, i.e. $T_{2ML} = 1.200/\eta^{0.9}$.

Oil Saturation

Low field NMR measurements were used to determine the oil saturation and oil viscosity for diatomite samples from the Belridge field, Kern County, California. The lab measurements were used to evaluate logs recorded on the well with an experimental logging tool, the CMR[2] Combinable Magnetic Resonance tool. The results of the log and lab measurements are described by Morriss et al [14].

The diatomite samples were measured three times. The first measurement was in their *native state* condition, i.e. prior to cleaning, at which time the pore fluids consisted of connate water, gas and native crude oils. The second was after displacing the gas with brine by placing the samples under brine with a light vacuum. Hence, differences between T_2-distributions from the first and second measurements, shown in Figure 18, indicate the volume of gas present at the time of the native state measurement.

The samples were then soaked in D_2O. During this procedure the D_2O diffuses into the sample and dilutes the concentration of H_2O to a negligible level. After repeated soaking, the remaining NMR signal originates entirely from the crude oil, since D_2O does not contribute an NMR signal at the operating frequency of the lab spectrometer. These T_2-distributions (Figure

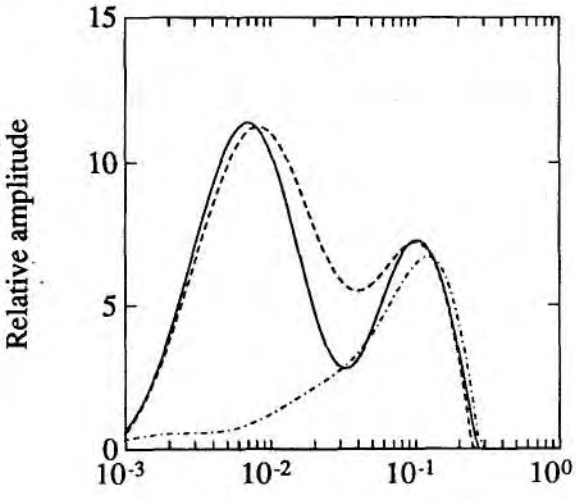

Figure 18: 2 MHz T_2-distributions for a diatomite sample. The difference between the native state material (solid) and the fully saturated samples (dashed) show gas saturation. The dash/dot curve is the distribution for oil measured after the H_2O signal was eliminated by dilution with D_2O.

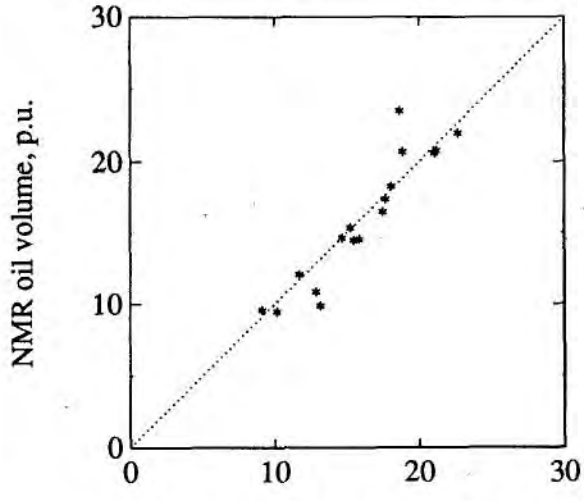

Figure 19: Comparison of oil volume determined by NMR with Dean-Stark extraction made subsequent to NMR analysis.

18) were found to be similar to T_2-distributions for the bulk oils. Hence, surface effects are not apparent; this indicates that the diatomite samples are predominantly water wet. Because of the absence of surface effects, oil viscosity can be estimated from T_{2ML} of the distribution,

[2]Mark of Schlumberger

using Figure 17.

Lastly, the NMR porosity after D_2O diffusion is a direct measure of the volume of oil in the sample, and was found to be in very good agreement with oil volumes determined from Dean-Stark extraction (Figure 19).

Conclusions

Low field NMR measurements can be obtained rapidly, in about 20 minutes, on both native state and cleaned samples. Although not as well established as other core testing methods, low field NMR is capable of quantifying a wide range of petrophysical properties with one nondestructive measurement.

- NMR measurements using low magnetic fields give accurate porosity values for both sandstones and carbonates. Low fields have $H\tau \leq 0.1$ gauss-sec.
- Low field T_2-distributions show good agreement with T_1-distributions and correspond to pore size distributions from mercury porosimetry.
- Free fluid porosities calculated using cutoffs of 33 and 92 msec for sandstones and carbonates, respectively, predict the producible fluid.
- In sandstones, clay bound water can be estimated from T_2 distributions using a 3 msec cutoff.
- Sandstone permeability can be estimated with $4.6T_{2ML}^2\phi^4$. For some vuggy carbonates, the NMR permeability estimate is improved by excluding the long-T_2 porosity that is associated with the vugs.
- Measurements on a large suite of crude oils and viscosity standards established that $T_{2ML} = 1.200/\eta^{0.9}$, where T_{2ML} is in seconds and η is in cp.
- Using D_2O diffusion, NMR can measure S_o and S_w in native state core. This method allows oil viscosity to be estimated in situ for water-wet rocks.

Acknowledgments

We would like to thank Phil Dryden at Schlumberger-Doll Research and Noel Patterson and John Ferris at Shell Development Co. for providing some of the experimental data. The NUMAR Corporation graciously provided Shell Deveopment Co. with the spectrometer that was used to make the 1 MHz measurements.

Nomenclature

A = signal amplitude
CEC = cation exchange capacity
D = diffusion constant of water
G = magnetic field gradient
H = magnetic field strength
k = permeability
M_n = net magnetization due to hydrogen
Q_{ve} = cation exchange capacity/pore volume
S = surface area
t = elapsed time
T = absolute temperature
T_1 = NMR longitudinal relaxation time constant
T_2 = NMR transverse relaxation time constant
T_{2ML} = NMR mean logarithmic T_2
T_{2B} = bulk fluid transverse time relaxation constant
T_{2S} = surface induced transverse relaxation time constant
V = volume
τ = Carr-Purcell pulse spacing, 1/2 the echo spacing in a CPMG
χ_e = electronic magnetic susceptibility
χ_n = nuclear magnetic susceptibility due to hydrogen
η = viscosity
γ = gyromagnetic ratio for hydrogen
ϕ = porosity

References

[1] M. N. Miller, Z. Paltiel, M. E. Gillen, J. Granot, and J. C. Bouton. Spin echo magnetic resonance logging: Porosity and free fluid index determination. In *Proceedings: SPE Annual Technical Conference*. Society of Petroleum Engineers, 1990. Paper 20561.

[2] R. L. Kleinberg, A. Sezginer, D. D. Griffith, and M. Fukuhara. Novel NMR apparatus for investigating an external sample. *J. Mag. Res.*, 97:466–485, 1992.

[3] C. E. Morriss, J. MacInnis, R. Freedman, J Smaardyk, C. Straley, W. E. Kenyon, H. J. Vinegar, and P. N. Tutunjian. Field test of an experimental pulsed nuclear magnetism tool. In *Trans. SPWLA Annu. Log. Symp.* Society of Professional Well Logging Analysts, 1993. Paper GGG.

[4] H. J. Vinegar, P. N. Tutunjian, P. T. Crabtree, F.J. Raffaldi, R. DiFoggio, and W. A. Edlestein. NMR spectroscopy of tight, gypsum-bearing carbonates. *The Log Analyst*, 32:527–533, September 1991. Originally presented at SPWLA 30th Annual Logging Symposium.

[5] R. J. S. Brown and P. Fantazzini. Conditions for initial quasi-linear T_2^{-1} vs τ for CPMG NMR with diffusion and susceptibility differences in porous media and tissues. *Phy. Rev. B*, 47:14823–14834, June 1993.

[6] N. Bloembergen, E. M. Purcell, and R. V. Pound. Relaxation effects in nuclear magnetic resonance absorption. *Phy. Rev.*, 73:679–712, 1948.

[7] M. H. Cohen and K. S. Mendelson. Nuclear magnetic resonance and the internal geometry of sedimentary rocks. *J. Appl. Phys.*, 53:1127–1135, 1982.

[8] R. L. Kleinberg, C. Straley, W. E. Kenyon, R. Akkurt, and S. A. Farooqui. Nuclear magnetic resonance of rocks: T_1 vs. T_2. In *Proceedings: SPE Annual Technical Conference.* Society of Petroleum Engineers, 1993. Paper 26470.

[9] W. E. Kenyon. Nuclear magnetic resonance as a petrophysical measurement. *Nucl. Geophys.*, 6:153–171, 1992.

[10] R.L. Kleinberg and Horsfield M.A. Transverse relaxation processes in porous sedimentary rock. *J. Mag. Res.*, 88:9–19, 1990.

[11] D. P. Gallegos and D. M. Smith. A NMR technique for the analysis of pore structure: Determination of continuous pore size distributions. *J. Col. I. Sci.*, 122(1):143–153, March 1988.

[12] E. J. Fordham, A. Sezginer, and L. D. Hall. Imaging multiexponential relaxation in the (y,$log_e(T_1)$) plane: Application to clay filtration in rock cores, 1994. Submitted to *J. Mag. Res.* for publication.

[13] R. Freedman. Processing method and apparatus for processing spin echo inphase and quadrature amplitudes from a pulsed nuclear magnetism tool and producing new output data to be recorded on an output record. U.S. Patent No. 5,291,137 issued March 1, 1994.

[14] C. E. Morriss, R. Freedman, C. Straley, M. Johnson, H. J. Vinegar, and P. N. Tutunjian. Hydrocarbon saturation and viscosity estimation from NMR logging in the Belridge Diatomite. In *Trans. SPWLA Annu. Log. Symp.* Society of Professional Well Logging Analysts, 1994. Paper C.

[15] C. Straley, C. E. Morriss, W. E. Kenyon, and J. J. Howard. NMR in partially saturated rocks: Laboratory insights on free fluid index and comparison with borehole logs. In *Trans. SPWLA Annu. Log. Symp.* Society of Professional Well Logging Analysts, 1991. Paper CC.

[16] H. H. Yuan and K. M. Diederix. The role of membrane potential measurements in shaly sand evaluation. In *Trans. SPWLA 28th Annu. Log. Symp.* Society of Professional Well Logging Analysts, 1987. Paper GG.

[17] H. J. Hill, O. J. Shirley, and G. E. Klein. Bound water in shaly sands - its relation to Q_v and other formation properties. *The Log Analyst*, 20:3–25, May 1979. Edited by M. H. Waxman and E. C. Thomas.

[18] G. A. LaTorraca, K. J. Dunn, and R. J. S. Brown. Predicting permeability from nuclear magnetic resonance and electrical properties measurements. In *Proceedings: SPE Annual Technical Conference.* Society of Petroleum Engineers, 1993. Paper 18272.

[19] D. Chang, H. J. Vinegar, C. E. Morriss, and C. Straley. Effective porosity, producible fluid and permeability in carbonates from NMR logging. In *Trans. SPWLA Annu. Log. Symp.* Society of Professional Well Logging Analysts, 1994. Paper A.